Study on the Structural Load-Bearing Capacity of Rectangular Reinforced Concrete Cable Channels with Corrosion Defects

Junbo Liu[1*], He Liu[1], Wei Wang[2], Jingyao Luan[1], Changlong Gao[1]

[1]State Grid Jilin Electric Power Research Institute, Changchun Jilin 130012, China
[2]State Grid Jilin Electric power supply company, Changchun Jilin 130022, China

*Corresponding author's email: 13894819779@139.com

Abstract. Reinforced concrete cable channels are highly susceptible to corrosion in underground environments, resulting in wall thinning. To explore the impact of corrosion-induced thinning on the residual load-bearing capacity of rectangular reinforced concrete cable channels, a Three-Point Bending (TEB) load-bearing capacity calculation model for rectangular reinforced concrete cable channels is proposed in this paper. The study contrasts corrosion depth with the protective layer thickness and establishes theoretical models for the residual load-bearing capacity of rectangular reinforced concrete cable channels with various corrosion depth defects. Subsequently, based on specific engineering cases, the paper calculates the load-bearing capacity of rectangular reinforced concrete cable channels with corrosion defects and validates the results through numerical simulations using ABAQUS. The findings demonstrate the feasibility of the proposed load-bearing capacity calculation model for rectangular reinforced concrete cable channels with corrosion defects.

Keywords: corrosion-induced thinning; structural load-bearing capacity; reinforced concrete material; rectangular; cable channel

1 Introduction

As China's modernization advances rapidly, urban electricity consumption and load have seen consistent growth. To address this, the use of ultra-high voltage cables for power transmission provides an effective solution to alleviate electricity consumption pressure. However, given their large outer diameter, considerable weight, and notable heat generation, traditional cable laying methods prove impractical for ultra-high voltage cables. Consequently, installing these cables within dedicated cable tunnels emerges as a viable solution, which not only effectively eases the challenge of urban land scarcity but also ensures the safety of both power facilities and urban residents [1-2].

Cable channels are commonly situated in soft soil layers within urban environments, subjecting them to intricate stress conditions that make them prone to defects such as

Q. Gao et al. (eds.), *Proceedings of the 2024 7th International Conference on Structural Engineering and Industrial Architecture (ICSEIA 2024)*, Atlantis Highlights in Engineering 30,
https://doi.org/10.2991/978-94-6463-429-7_44

corrosion and cracks. Moreover, with prolonged usage, the materials may undergo degradation, introducing potential safety hazards [3]. Systematic inspections of operational cable channel structures, coupled with theoretical load-bearing capacity calculations derived from inspection parameters, offer a scientific foundation for assessing the safety of cable channel structures. Additionally, this approach serves as a theoretical foundation for subsequent maintenance, repair, and renovation efforts [4].

Rectangular cable channels are essentially non-homogeneous thick-walled tubular components, predominantly made of reinforced concrete materials. The calculation methods for determining the load-bearing capacity of oil and gas steel pipes after corrosion typically involve approaches like elastic-plastic mechanics and semi-empirical formulas related to fracture mechanics. While these methods are relatively well-established and straightforward, their applicability to rectangular cable channels is limited due to differences in material composition and sectional shape [5-8]. Presently, in global research on the load-bearing performance of corroded reinforced concrete thick-walled tubular components, scholars commonly consider the influence of microscopic particle concentration and diffusion patterns, such as chloride ions, on the compressive strength of concrete, along with the compressive and tensile strength of reinforcing steel [9]. While these studies accurately depict the corrosive solution's mechanisms on reinforced concrete materials, there exists a research gap concerning the overall stress characteristics of reinforced concrete composite components under corrosive conditions [10].

In summary, there is limited research on the load-bearing performance of reinforced concrete materials, especially non-homogeneous thick-walled tubular components like cable channels, after experiencing extensive corrosion-induced thinning. This paper endeavors to establish a load-bearing capacity calculation model for cable channels affected by corrosion-induced thinning, subsequently validating it through numerical simulation methods and engineering case studies.

2 TEB load model for rectangular cable channels

For reinforced concrete pipe segments with circular sections, their load-bearing capacity is typically determined through three-point bending (TEB) tests in accordance with relevant experimental standards. Although specific testing standards for rectangular pipe segments are lacking, domestic manufacturers also utilize TEB tests to ascertain the load-bearing capacity of rectangular reinforced concrete pipe segments. The load-bearing capacity determination for cable channels with rectangular sections can draw upon testing methods employed for rectangular pipe segments. The force diagram for cable channels under TEB testing is illustrated in Figure 1.

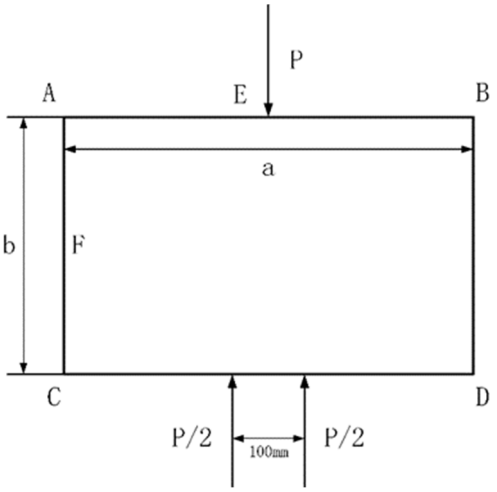

Fig. 1. Force diagram for the rectangular cable channel.

Figure 2 illustrates the process of simplifying the force distribution of cable channels, and the simplified model assumes an axially symmetrical structure. This symmetrical shape considers 1/4 of the component for calculations. Points E and F, located on the axis of symmetry, exhibit vertical and lateral displacements, respectively. Consequently, points E and F can be simplified by imposing sliding constraints, leading to the simplified force diagram shown in Figure 3.

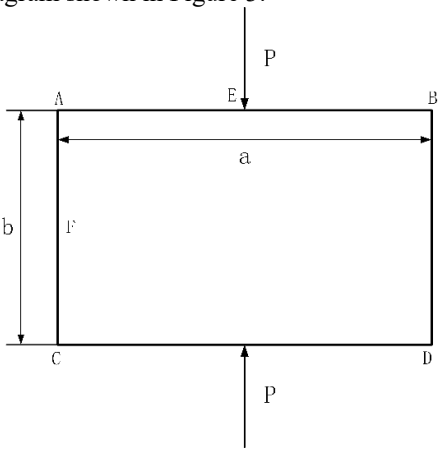

Fig. 2. Simplified force diagram for the cable channel.

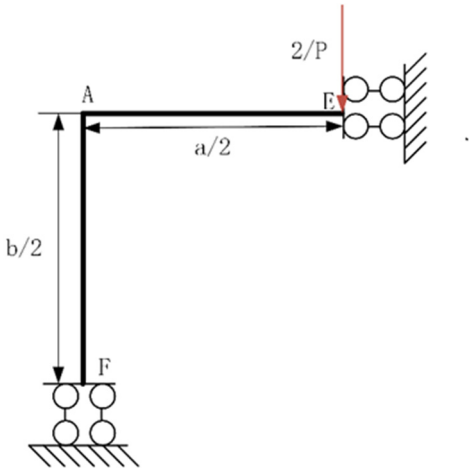

Fig. 3. Force diagram for 1/4 structure.

According to the displacement method, the MEA for the simplified structure can be determined as follows:

$$\begin{cases} M_{AE}=i_1\theta_A-\dfrac{Fa}{8} \\ M_{AF}=i_2\theta_A \\ M_{EA}=-i_1\theta_A-\dfrac{Fa}{8} \end{cases} \tag{1}$$

Given that $M_{AF}+M_{AE}=0$, the solution is:

$$\theta_A=\frac{Fa}{8(i_1+i_2)} \tag{2}$$

$$\begin{cases} M_{AE}=-\dfrac{Fa^2}{8(a+b)} \\ M_{AF}=\dfrac{Fa^2}{8(a+b)} \\ M_{EA}=-\dfrac{(2Fab+Fa^2)}{8(a+b)} \end{cases} \tag{3}$$

In this equation: θ represents the rotational angle; a denotes the length of the cable channel cross-section in meters (m); b is the width of the cable channel cross-section in meters (m); F stands for the line load (N); i represents the line stiffness, where $i=\frac{EI}{l}$.

$$F=\frac{8M_{EA}(a+b)}{2ab+a^2} \tag{4}$$

Therefore, the ultimate load-bearing capacity of the cable channel can be determined by calculating the maximum bending moment at the section where the rotation occurs:

The relationship between the load borne by the cable channels in a TEB test and the bending moment at the cross-section where rotation occurs is given by:

$$F_{max}=\frac{8M_{max}(a+b)}{2ab+a^2} \tag{5}$$

Cable channels typically utilize a double-layer reinforcement approach. In the event of a cable channel failure, the upper section experiences compression, while the lower section undergoes tension. Considering a small segment at point A as an isolation body, the sectional front view and side view are depicted in Figure 4.

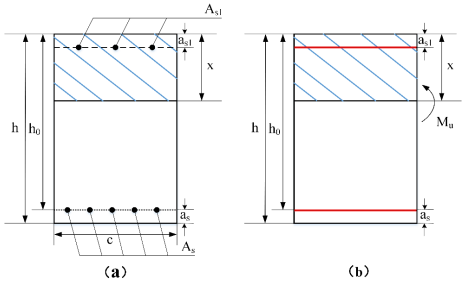

Fig. 4. Front view (a) and side view (b) of the isolation body.

Based on the equilibrium conditions of forces, the following can be derived:

$$\alpha_1 f_{cc} cx+f_{rc}A_{s1}=f_{rt}A_s \tag{6}$$

Then, the height of the compressed zone can be expressed as:

$$x=\frac{f_{rt}A_s-f_{rc}A_{s1}}{\alpha_1 f_{cc}c} \tag{7}$$

Calculating the moment of the resultant force exerted on the compressed reinforcing steel yields the following expression:

$$M_u=\alpha_1 f_{cc}cx\left(h_0-\frac{x}{2}\right)+f_{rc}A_{s1}(h_0-a_{s1}) \tag{8}$$

By substituting the value of x into Equation (8), the following can be obtained:

$$M_u=(f_{rt}A_s-f_{rc}A_{s1})\left(h_0-\frac{f_{rt}A_s-f_{rc}A_{s1}}{2\alpha_1 f_{cc}c}\right)+f_{rc}A_{s1}(h_0-a_{s1}) \tag{9}$$

In the equation, M_u signifies the maximum bending moment sustained by the section, measured in N·mm; f_{rt} and f_{rc} denote the tensile and compressive strengths of the circumferential reinforcement, respectively, expressed in MPa; f_{cc} represents the compressive strength of concrete in MPa; A_s and A_{s1} indicate the sectional areas of tensile and compressive steel reinforcements, measured in mm²; x represents the height of the compressed zone in mm; h_0 is the effective height in mm, where $h_0 = h - a_s$; h and c refer to the calculated section height and width in mm; a_s and a_{s1} represent the thickness of the protective layer inside and outside the cable duct, respectively, measured in mm; α_1 is the coefficient for the equivalent rectangular stress diagram in the compressed concrete zone, with a value of 1.0 for concrete grades up to C50.

Upon the occurrence of failure in the pipe segment subjected to TEBT loading, we yield:

$$M_u=M_{A,\,max} \tag{10}$$

By combining Equations (5), (9), and (10), the maximum load-bearing capacity of the reinforced concrete pipe segment under TEB conditions can be determined as follows:

$$F_{max} = \frac{8\left((f_{rt}A_s - f_{rc}A_{s1})\left(h_0 - \frac{f_{rt}A_s - f_{rc}A_{s1}}{2\alpha_1 f_{cc}c}\right) + f_{rc}A_{s1}(h_0 - a_{s1})\right)(a+b)}{a^2 + 2ab} \quad (11)$$

In the equation: F_{max} represents the maximum load capacity of the cable channel in N; a and b denote the length and width of the cable channel, respectively, measured in mm.

3 Residual load-bearing capacity model for cable channels with corrosion defects

Corrosion effects on reinforced concrete components generally manifest in four aspects: deterioration of concrete material, corrosion of reinforcing steel, corrosion-induced thinning of structural components, and a weakening of the interaction between concrete and steel. Equation (11) is derived to establish the model for the maximum load-bearing capacity of undamaged cable channels. Considering the influence of corrosion on reinforced concrete components, the following assumptions can be formulated:

(1) The deterioration of concrete material is typically characterized by a reduction in compressive strength or a decrease in the elastic modulus. To articulate this transformation, a concrete strength reduction factor, denoted as k_c, is introduced. The determination of k_c can be achieved through relevant indoor tests;

(2) Corrosion of reinforcing steel results in the loss of steel quality and section, leading to reduced yield strength and tensile strength. To describe this alternation, a corrosion reduction factor for reinforcing steel, indicated as k_r, is put forth. The value of k_r is associated with variations in the sectional area of reinforcing steel and changes in tensile strength. Both factors can be determined through indoor tests;

(3) Corrosion-induced thinning of structural components brings about variations in component thickness. This thinning in reinforced concrete pipe components is typically analyzed in two scenarios. If the thickness of corrosion-induced thinning is less than that of the protective layer, it is conceivable that the dimensions of the reinforced concrete pipe component have changed, accompanied by a mere reduction in the tensile strength of the concrete portion. However, should the thickness of corrosion-induced thinning exceed that of the protective layer, it leads to a decrease in the compressive tensile strength of the concrete, consequently significantly diminishing the load-bearing capacity of the components.

(4) The interaction between concrete and reinforcing steel involves both mechanical interlocking forces and bonding strength. The bonding strength at the interface of concrete and reinforcing steel can be evaluated through direct shear tests. To account for this, a bond strength reduction factor kcr is introduced. The value of this factor is influenced by the post-corrosion strength of the reinforcing steel, concrete strength, and the bonded area between reinforcing steel and concrete.

(5) When the thickness of corrosion-induced thinning is less than the protective layer thickness, calculations can be performed using the bond strength reduction factor (k_{cr}) at the interface between concrete and reinforcing steel. However, when the thickness of corrosion-induced thinning exceeds that of the protective layer, notable alterations in the forces acting between reinforcing steel and concrete become apparent.

Based on the aforementioned assumptions, the maximum bending moment that a double-reinforced rectangular section can withstand after corrosion is determined as follows:

$$M_{u1}=\begin{cases} k_{cr}\left(\alpha_1 k_c f_{cc} c x_1\left(h_0-\frac{x_1}{2}\right)+k_r f_{rc} A_{s1}(h_0-a_{s1})\right) & d\le a_s \\ k_{cr}\left(\alpha_1 k_c f_{cc} c x_1\left(h-\frac{x_1}{2}-d\right)+k_r f_{rc} A_{s1}(h-a_{s1}-d)\right) & d>a_s \end{cases} \tag{12}$$

Among them:

$$x_1=k_r\frac{f_{rt}A_s-f_{rc}A_{s1}}{\alpha_1 f_{cc} c}=k_r x \tag{13}$$

In the equation: M_{u1} represents the maximum bending moment sustained by the corroded reinforced concrete pipe segment section, measured in N·mm; k_c and k_r are the reduction factors for the compressive strength of the corroded concrete and reinforcing steel (with the approximation that the reduction in tensile strength of the reinforcing steel is equivalent to the reduction in compressive strength); k_{cr} signifies the reduction factor for the bonding strength between concrete and reinforcing steel; d denotes the corrosion depth, measured in mm; and x_1 represents the height of the compressed concrete zone in the corrosion-induced thinning section, measured in mm. Other parameters maintain the same meanings as defined in Equation (9).

Similarly, the subsequent equation is executed:

$$M_{u1}=M_{A,\max} \tag{14}$$

By combining Equations (5), (12), and (14), the maximum load that the concrete pipe segment with corrosion defects can withstand under TEB conditions can be determined:

$$F_{max1}=\begin{cases} \dfrac{8k_{cr}\left(\alpha_1 k_c f_{cc} c x_1\left(h_0-\frac{x_1}{2}\right)+k_r f_{rc} A_{s1}(h_0-a_{s1})\right)(a+b+2d)}{(a+2b+3d)(a+d)} \\ \dfrac{8k_{cr}\left(\alpha_1 k_c f_{cc} c x_1\left(h-\frac{x_1}{2}-d\right)+k_r f_{rc} A_{s1}(h-a_{s1}-d)\right)(a+b+2d)}{(a+2b+3d)(a+d)} \end{cases} \tag{15}$$

In the equation: F_{max1} represents the residual load-bearing capacity of the corroded reinforced concrete pipe segment.

4 Case study

The case study involves the cast-in-place pipe segment within the comprehensive pipe gallery at Huanggang Mingzhu Avenue, with various parameters specified in Table 1. The primary focus of this study is to examine the influence of corrosion depth on the load-bearing performance of the cable channel, excluding considerations for the reduction in material mechanical properties due to corrosion. In Equation (15), the reduction factors k_r and k_c for reinforcing steel and concrete, along with k_{cr} for the bonding strength between reinforcing steel and concrete, are all assumed to be 1.

By substituting the parameters from the table into Equation (11), the load-bearing capacity of the undamaged rectangular reinforced concrete cable channel is calculated to be approximately 799.41 kN. When the corrosion depth reaches 40 mm, the inner stirrups of the cable channel become exposed to the air. At this juncture, the calculated load-bearing capacity is approximately 791.99 kN.

According to Figure 5, it is evident that the load-bearing performance of the cable channel linearly decreases with the increase in corrosion depth along the inner wall. When the corrosion depth reaches 40 mm, the protective layer on the inner side of the cable channel is entirely corroded. At this point, the reduction in the load-bearing capacity of the cable channel is approximately 0.93%. As the corrosion depth surpasses the thickness of the inner protective layer, reaching 72 mm, the reinforcing steel cage is completely exposed to the air. At this stage, the calculated ultimate load-bearing capacity of the cable channel is 693.79 kN, representing a reduction of approximately 13.21%.

Table 1. Performance parameters of the reinforced concrete pipe segment.

Pipe segment parameters	Values	Pipe segment parameters	Values
Mean length A/mm	4400	Stirrup tensile strength F_{rt}/mpa	650
Mean width B/mm	3700	Stirrup compressive strength F_{rc}/mpa	613
Pipe length C/mm	1000	Stirrup diameter D_l/mpa	16
Wall thickness H/mm	350	Number of stirrup loops	10
Inner protective layer thickness A_s/mm	40	Tensile steel area A_s/mm^2	3617.28
Outer protective layer thickness A_{s1}/mm	50	Compressive steel area A_{s1}/mm^2	1808.64
Concrete compressive strength F_{cc}/mpa	23.4		

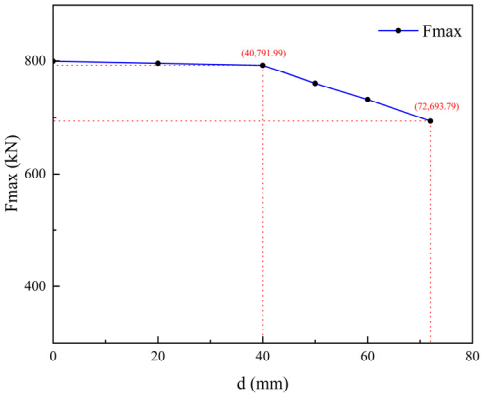

Fig. 5. Fmax-d curve with theoretical calculation.

In practical scenarios, when the inner reinforcing steel is fully disengaged from the cable channel, the cable channel transforms into a single-reinforcement component. This alteration in the structural configuration results in changes to the loading conditions at the critical section, leading to adjustments in parameters such as compressive zone height and internal force of the reinforcing steel. Consequently, it becomes necessary to re-derive the formulas. The derivation process is detailed below:

From the equilibrium condition for the moment in a single-layer reinforcement section, the following can be obtained:

$$\alpha_1 f_{cc} cx = f_{rt} A_{s1} \tag{16}$$

The compressed zone is calculated by the following equation:

$$x = \frac{f_{rt} A_{s1}}{\alpha_1 f_{cc} c} \tag{17}$$

By taking the moment about the resultant force acting on the compressed reinforcement, and substituting the value of x, the following can be obtained:

$$M_u = f_{rt} A_{s1} \left(h\text{-}d\text{-}\frac{f_{rt} A_{s1}}{2\alpha_1 f_{cc} c} \right) \tag{18}$$

By combining Equations (5), (10), and (18), the maximum load-bearing capacity of the reinforced concrete cable channel under TEB loading conditions can be determined when the corrosion depth exceeds the protective layer thickness:

$$F_{max} = \frac{8 f_{rt} A_{s1} \left(h\text{-}d\text{-}\frac{f_{rt} A_{s1}}{2\alpha_1 f_{cc} c} \right) (a+b+2d)}{(a+2b+3d)(a+d)} \tag{19}$$

With the incorporation of the corrosion reduction factors, the aforementioned equation can be expressed as follows:

$$F_{max} = \frac{8 k_{cr} k_c f_{rt} A_{s1} \left(h\text{-}d\text{-}\frac{f_{rt} A_{s1}}{2\alpha_1 f_{cc} c} \right) (a+b+2d)}{(a+2b+3d)(a+d)} \tag{20}$$

When the corrosion depth exceeds 72 mm, the inner reinforcing steel is completely exposed, causing the originally externally compressed steel to become tensioned. The height of the compressed zone (x) undergoes a corresponding change. Subsequently, by applying the data from the table to Equation (20), the calculated maximum load-bearing capacity of the cable channel is approximately 365.05 kN. This strength represents only 45.66% of the intact reinforced concrete cable channel, signifying a reduction in strength by over half. In this context, the obtained results demonstrate a closer alignment with real-world conditions when contrasted with the outcomes derived from the load-bearing capacity calculation equation for double-layer reinforced concrete cable channels.

5 Numerical simulation analysis of load-bearing capacity in rectangular cable channels with corrosion-induced thinning

The load-bearing capacity of rectangular reinforced concrete cable channels was simulated under both undamaged conditions and corrosion-induced thinning conditions using the ABAQUS finite element analysis software. The model setup steps are outlined as follows:

(1) Model construction: The model is developed in accordance with the design drawings, maintaining consistency in dimensions, internal placement of reinforcing steel, and other parameters specified in the design drawings. This process is illustrated in Figure 6, where concrete elements are represented as three-dimensional solids, and the reinforcing steel is depicted as linear elements;

(2) Material property: Reinforcing steel is characterized by an elastic-plastic model, while concrete employs a plastic damage model;

(3) Component assembly: The embedded region constraint approach is utilized to assemble the reinforcing steel and concrete components;

(4) Establishment of analysis steps: After setting up the static force analysis steps, the continuous reduction frequency of incremental steps is adjusted, and the history output of reference points is established to extract loads and displacements in the Y-direction;

(5) Definition of constraints and application of loads: Full fixed constraints (U1=U2=U3=UR1=UR2=UR3) are implemented at the bottom of the component in the force-bearing region. A uniform surface load is applied at the top using the displacement coupling method;

(6) Mesh partitioning: The mesh partitioning of the component is illustrated in Figure 6, and the analysis is subsequently submitted for resolution.

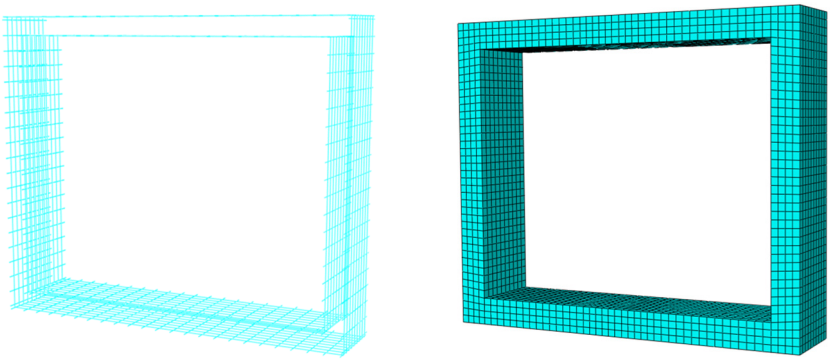

(a) Reinforcing steel cage mesh. (b) Concrete component model.

Fig. 6. Schematic diagram of the component model.

The numerical simulation corresponds to the dimensional parameters of the cable channel, as presented in Table 2:

Table 2. Corresponding dimensional parameters for each group in numerical simulation.

Corrosion Depth d/mm	Pipe Length c/mm	Wall Thickness h/mm	Mean Length a/mm	Mean Height b/mm
0	1000	350	4400	3700
20	1000	330	4380	3780
40	1000	310	4360	3760
50	1000	300	4350	3750
60	1000	290	4340	3740
72	1000	278	4328	3728

Among them, the first group represents the undamaged pipe segment. The cable channel with corrosion defects is achieved by adjusting the model parameters. When the corrosion depth exceeds 40 mm, the inner reinforcing steel is exposed. To prevent non-convergence issues during the model calculation process, the inner reinforcing steel cage is removed, and the simulation results are compared with the calculated results.

The comparison between the simulation results and the theoretical model calculations is shown in Figure 7. It can be perceived that when the corrosion depth does not exceed the depth of the inner protective layer (d≤40 mm), the model-calculated maximum load-bearing capacity of the cable channel closely aligns with the simulated values, with an error controlled within 5%. The simulated values are slightly larger than the theoretical calculations. However, when the corrosion depth exceeds the protective layer thickness (d＞40 mm), the error between theoretical values and simulated values exceeds 90%. At this point, Equation (15) is no longer applicable. By comparing the simulated values with the corrected values, it becomes evident that the corrected values are more accurate than the theoretical values, with errors within 10%. This discrepancy arises because, as the corrosion depth surpasses the thickness of the inner protective layer, the bonding strength between the reinforcing steel and concrete significantly decreases. With increasing depth of corrosion, the inner reinforcing steel gradually disengages from the component. Neglecting the influence of the inner reinforcing steel in the calculation brings the theoretical results closer to the numerical simulation outcomes.

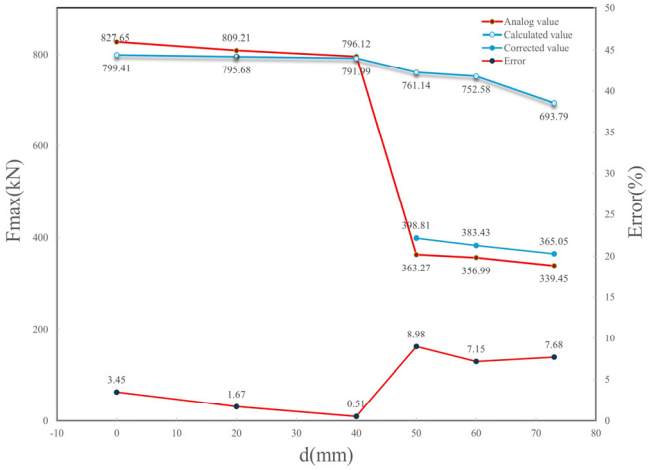

Fig. 7. Comparison curves between simulation results and theoretical model.

6 Conclusion and outlook

The primary conclusions drawn from this study are as follows:

(1) By analyzing the force and section bending of rectangular reinforced concrete cable channels, a formula for the maximum load-bearing capacity of double-layer reinforced components in TEB tests was derived. Subsequently, a quantitative relationship between the ultimate load-bearing capacity of components with corrosion thinning defects and the corrosion depth was deduced.

(2) The accuracy of the model was validated using numerical simulation methods. Stress distribution in the cable channel was verified for both non-corroded and various corrosion depth scenarios. Stress cloud maps and plastic strain cloud maps were generated to compare the theoretically calculated values with the simulated values of the component's maximum load-bearing capacity. The results indicate that when the corrosion depth is less than the protective layer thickness, the numerical simulation results closely align with the theoretically calculated values for double-reinforced components. When the corrosion depth exceeds the protective layer thickness, the numerical simulation results are more consistent with the theoretically calculated values for single-reinforced components, with errors controlled within 10%.

(3) In this study on the load-bearing performance of reinforced concrete cable channel components with corrosion defects, the reduction in material strength under corrosion conditions was disregarded. Future research endeavors should address this omission by conducting scaled-down experiments and material performance tests. All material constitutive parameters employed in the numerical simulation process were derived from the tests. Moreover, the force conditions acting on cable channels are inherently intricate, and a more realistic approach to calculating the ultimate load-bearing capacity would involve accounting for soil loads and live loads.

Acknowledgment

This paper is supported by the project of State Grid Jilin Electric Power Research Institute: Research on Cable Channel Structure Detection (KY-GS-21-01-12).

References

1. Li M., He L., Ma B. S., et al. Structure failure and rehabilitation technologies of the cable tunnel [J]. Bulletin of Geological Science and Technology, 2020, 39(5): 31-37.
2. Sterling R L .Developments and Research Directions in Pipe Jacking and Microtunneling[J].Underground Space, 2018, 5(1): 1-19.
3. Jiang Y. J., Xu Y., Chen P., et al. Discussion on the defects and its inspection and evaluation methods for power cable tunnels [J]. Chinense Journal Undergrond Space Engineering, 2019, 15(1): 311-318.
4. Zhu Y. X. Research progress in applicability evaluation technology for defective pipelines [J]. Chemical Engineering & Machinery, 2014, 41(1): 16-19.

5. Du G. F., Zhang D. S., Liu G. J., et al. Tresca yield criterion-based residual strength calculation of even corrosion pipeline [J]. China Petroleum Machinery, 2013, 41(4): 106-109.
6. Fu D. M., Sun J. A new method to predict residual strength of corrosion pipelines [J]. Oil & Gas Storage and Transportation, 2004, 23(4): 12-18.
7. Yu X. C., Hu Y. Q., Zhao J. Z., et al.. A study of calculating methods for residual strength of corrosion pipelines [J]. Acta Mechanica Sinica, 2004, 36(3): 281-287.
8. Liu S. C. Durability analysis of hydraulic concrete structure under chloride erosion environment [J]. Hydraulic Science and Technology, 2013, 4: 56-58.
9. Zhang Q., Guo L. Simulation of nonlinear corrosion damage process in reinforced concrete under chloride environment [J]. Journal of Hunan University Natural Sciences, 2017, 44(5): 44-52.
10. Moradi M., Valipour H., Foster S. Reserve of Strength in Inverted U-Shaped RC Culverts: Effect of Backfill on Ultimate Load Capacity and Fatigue Life[J]. Journal of Bridge Engineering, 2016, 21(2):04015051.1-04015051.10.